

sorbent particles in an optical tweezer [5]. Applications to trap atoms have also been proposed [6].

In the acoustic context, \mathbf{V} can occur either in the linear or nonlinear regime [7], [8]. Considering that several researchers have found analogies between the structure of screw dislocations and vortices in fluids and quantum mechanics, the \mathbf{V} has been proposed as a tool for the experimental study of their optical, fluidic, and quantum counterparts. Recently the transfer of angular momentum from rotating acoustic waves to matter has been experimentally demonstrated by using several sound sources [9], [10]. Another interesting property of \mathbf{V} is the storage and transmission of digitized information with the particularity that the phase coding is in space and not in time [11]. Even though the potential of use of \mathbf{V} has been reported, their application in acoustics has been scarce.

I. I

Phase distribution singularities constitute an intrinsic characteristic of a given acoustic field. This type of feature occurs naturally in a wavefront and is known to be resistant to disturbances in the field [1]. In general, phase singularities, depending on the morphology of the dislocation, can be axial, screw-type, or mixed. Particularly, in this work we focused on screw dislocations, in which the transverse plane of the wavefront, normal to the propagation axis, exhibits a phase distribution which linearly increases from 0 to 2π over any circular trajectory around the principal axis. Fig. 1 shows a spatial representation of a beam with a screw dislocation, also known as a helical wave.

Because of the great similarity between a helical wavefront and vortices in a fluid, pressure fields with screw dislocation are also known as acoustic vortices [1]. Indeed, under special conditions, the interaction between vortices of this type resembles that of their fluid counterparts. Although the existence of a wavefront with screw dislocation was first identified acoustically, most of the subsequent research and applications has been reported in the optics field [3]. In this sense, it has been demonstrated that a helical wavefront transports angular momentum [4], which makes it possible to control the orientation of ab-

sorption instrumentation to generate a helical wavefront. Thus far, different methods for \mathbf{V} generation have been proposed, namely, direct generation from a specially shaped source [7], [12], the optoacoustic technique [13], mode conversion from wave plane to \mathbf{V} [9], or use of a phased array system [11].

Ferroelectret technology exhibits interesting properties which make it an excellent candidate to satisfy the current demand for the development of airborne ultrasonic transducers. In particular, cellular ferroelectrets open up new possibilities at the transducer design stage, to approach the trade-off among bandwidth, directivity, sensitivity, and cost. This is possible because of their high piezoelectric coefficient; wide frequency range of operation (from 30 kHz to 2 MHz); low acoustic impedance (< 0.03 MRayls), which results in a good adaptation to the air; and their unprecedented mechanical flexibility. Furthermore, ferroelectrets are easy to use and have a low fabrication cost [14] [16]. In this work, we propose a fast and inexpensive alternative for the creation of acoustic vortices by gluing a ferroelectret film onto a tangential/helical surface substrate. The high mechanical flexibility of this material allows us to fabricate transducers on any developable surface. (A developable surface is any sur-

L. Ealo is with the University of Valle, School of Mechanical Engineering, Cali, Colombia (e-mail: joao.ealo@correounivalle.edu.co).

J. C. Prieto and F. Seco are with the Centre of Automation and Robotics, Consejo Superior de Investigaciones Científicas (CSIC), Universidad Politécnica de Madrid (UPM), Systems Department, Madrid, Digital Object Identifier 10.1109/TUFFC.2011.1992

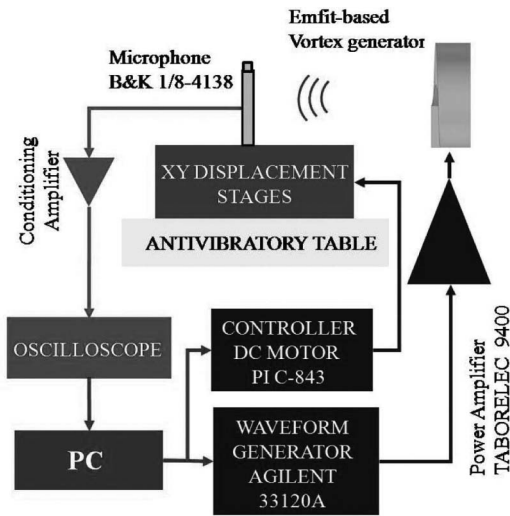


Fig. 3. Instrumentation setup.

$$(r, \phi, z) = A(r, \phi, z) \exp(i(m\phi - \omega t)), \quad (1)$$

where

$$p_{n,m}(r, \phi, z) = E(r, z) G_{n,m}(r, z) \exp(i(m\phi - \omega t)) \quad (2)$$

is the pressure distribution at a plane normal to the propagation axis. The functions $E(r, z)$, $G_{n,m}(r, z)$, and $\exp(i(m\phi - \omega t))$ are, respectively, the envelope of the beam (usually assumed to be Gaussian), the amplitude distribution near the core of the vortex, the beam phase structure, and the Gouy's phase.

A Gaussian envelope of the beam is given by

$$A(r, z) = \frac{1}{(1 + z^2/R^2)^{1/2}} \exp\left(-\frac{r^2}{2(z + \sqrt{z^2 + R^2})}\right) \exp\left(-\frac{z^2}{2(z + \sqrt{z^2 + R^2})}\right), \quad (3)$$

where A is a normalization constant, $R = kw_0^2/2$ is the Rayleigh's distance (w_0 is the width of the beam at $z = 0$ and k is the wavenumber), and $w(z) = w_0[1 + (z/R)^2]^{1/2}$ represents the width distribution of the beam throughout the propagation path.

Pressure distribution close to the core of the beam is given by

$$G_{n,m}(r, z) = \left(\frac{r\sqrt{z + \sqrt{z^2 + R^2}}}{w(z)}\right)^{|m|} L_{n-|m|}^{|m|} \left(\frac{r^2}{w(z)^2}\right) \quad (4)$$

where $L_{n-|m|}^{|m|}$ are the Laguerre's generalized polynomials [20] of radial index $n = |m|, |m| + 2, |m| + 4, \dots$, and $\exp(i(m\phi - \omega t))$ is the phase structure of the beam with topological charge m .

The helical structure of the beam phase results from the term:

$$\Phi(\phi) = \exp(im\phi), \quad (5)$$

and the Gouy's phase reads [7], [21]:

$$\psi(z) = \arctan\left(\frac{z}{R}\right) \quad (6)$$

where $\psi(z) = \arctan(z/R)$.

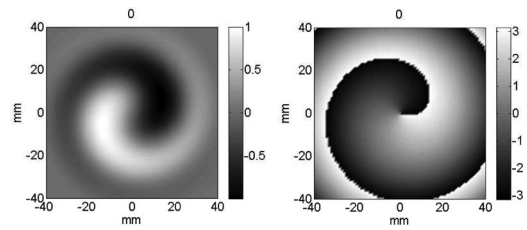


Fig. 4. Instantaneous Gaussian helical field. Simulation results using a topological charge $m = 1$. Left: pressure magnitude, right: phase.

Fig. 5. Instantaneous Gaussian helical field. Simulation results using a topological charge $m = 3$. Left: pressure magnitude, right: phase.

Eq. (1) enables us to synthesize a Gaussian beam corresponding to a phase singularity in the wavefront and propagating with time at any observation plane parallel to the vortex generator transducer. This result, used frequently to model an optical helical beam, is employed in the next section to qualitatively compare the structure of the screw dislocation obtained from theoretical simulation with that measured at the observation planes. Figs. 4 and 5 show the instantaneous pressure field of a Gaussian beam and its respective phase distribution, for two different topological charges, i.e., $m = 1$ and $m = 3$. Note that phase varies between π rad and 3π rad as we follow a circular trajectory around the core of the vortex; finding one and three discontinuities respectively.

Considering that the Gaussian beam formulation is not satisfactory to model the near field pattern of a finite source generating a helical beam, we have also used the well-known distributed point source method [22] to numerically predict the acoustic field produced by the fabricated prototype, as shown in Fig. 6.

IV. RESULTS: HELICAL WAVES

In this section, we demonstrate that gluing a ferroelectric film on a developable surface allows us to generate a customizable acoustic radiating pattern. In particular, we show that it is possible to create an acoustic vortex using a tangential surface substrate. Empirical and theoretical simulation results are compared to evaluate the quality of the generated helical wavefront at two different planes of observation. We applied a sinusoidal burst of 10 cycles at a frequency of 100 Hz, using a low pulse repetition frequency to avoid the creation of a standing wave. Figs. 7 and 8 show the measured and estimated acoustic pressure fields, at 100 and 200 mm, respectively, at 4 different

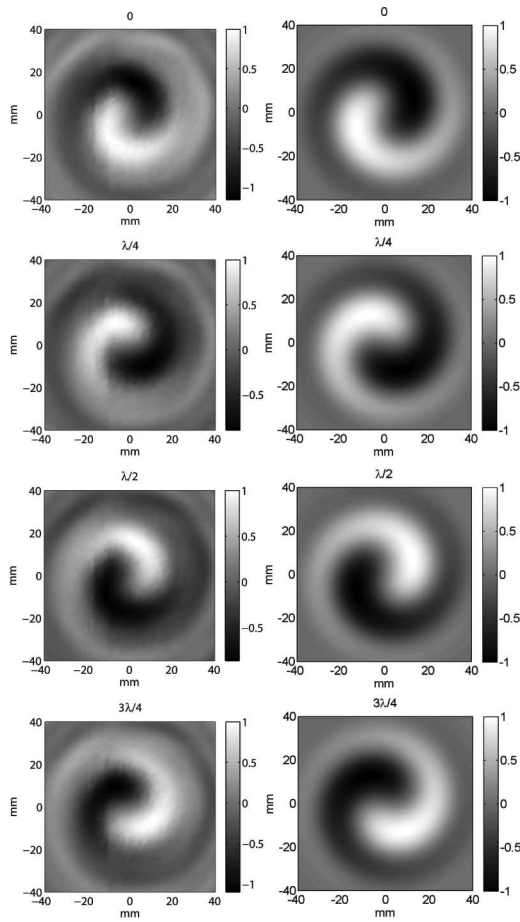


Fig. 8. Normalized instantaneous pressure amplitude at an observation plane located 200 mm from the transducer. Four different instants within a period of oscillation τ are shown ($0, \pi/4, \pi/2, 3\pi/4$). Topological charge $m = 1$, left: measured acoustic vortex, right: synthesized Gaussian beam ($\varphi_0 = 13 \text{ mm}$, $z = 200 \text{ mm}$).

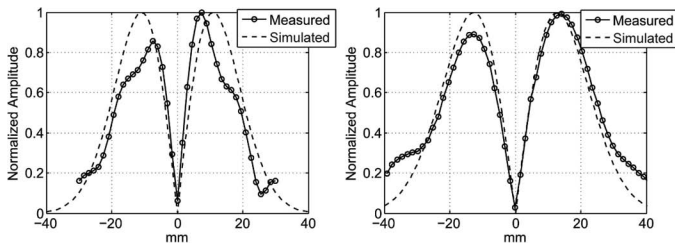


Fig. 9. Comparison between the envelope of a Gaussian beam and that of the acoustic vortex generated with the ferroelectret-based transducer. Left: at the observation plane ($X, 100 \text{ mm}$), i.e., in the near field of the vortex generator; right: at the observation plane (200 mm).

Experimental results obtained were in excellent agreement with theoretical estimations which indicates that it is possible to generate high-quality helical wavefronts easily and reliably. This paves the way for the potential use of multi-acoustic vortices in engineering applications without using a complicated setup to produce them. Considering that the sensitivity of the ferroelectret films is moderate (around 15 to 20 dB lower than that of resonant piezoceramics and PVDF-based transducers), the excitation voltage and

Fig. 10. Normalized magnitude (top panel) and phase (low pane) of a helical wavefront at an observation plane located at a distance of 100 mm from the transducer. Maximum pressure obtained: $P_a = 3.7 \text{ Pa}$, frequency = 100kHz. Topological charge $m = 1$. Left: measured acoustic vortex, right: simulated using the distributed point source model method.

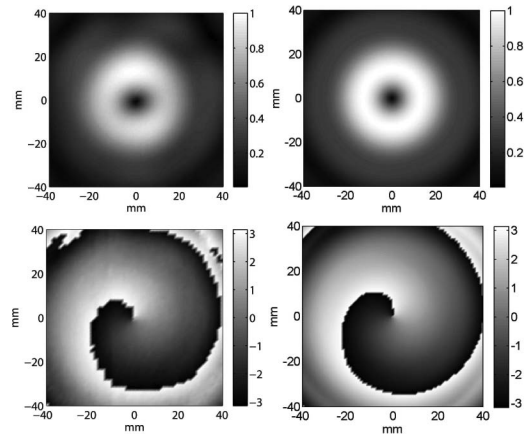


Fig. 11. Normalized magnitude (top panel) and phase (low pane) of a helical wavefront at an observation plane located at a distance of 200 mm from the transducer. Maximum pressure obtained: $P_a = 9.8 \text{ Pa}$, frequency = 100kHz. Topological charge $m = 1$. Left: Measured acoustic vortex, right: simulated using the distributed point source model method.

the size of the vortex generator must be properly chosen to obtain the desired acoustic output. However, its wide frequency range of operation, from 20 kHz to several hundreds of kilohertz, which allows us to create vortices of different topological charge using the same transducer, and its ease of use make the ferroelectret technology an excellent candidate for ultrasonic vortex generation. Further research is required to quantify the effect of the variations in the piston-like response of the film at frequencies beyond 150 kHz on the generated acoustic vortices. It is important to point out that the ultrasonic vortex can also be achieved using a ferroelectret-based multi-transducer along a phased-array system. In this manner, the phase singularity is created not by using a helical surface but electronically. An easy procedure to fabricate ferroelectret-based multi-transducers has recently been demonstrated [23].

Fig. 12. Time variation of the acoustic pressure of 51 different points deployed on a line that transversely crosses the helical wavefront measurement plane (X, Y, 200mm). The spacing of the observation points was 1.6 mm. Left: time responses arranged vertically, right: top view of the pressure distribution.

Fig. 13. Time evolution of the ultrasonic vortex. Plotted dots correspond to the points with constant phase measured on a grid covering the plane (X, Y, 200mm). The spacing between the elements of the grid is 1.6 mm.

R

- [1] J. F. Nye, *Natural Focusing and Fine Structure of Light*, Bristol, UK: IOP Publishing, 1999.
- [2] D. Rozas, C. T. Law, and G. A. Swartzlander, Experimental observation of fluidlike motion of optical vortices, *Phys. Rev. Lett.*, vol. 79, no. 18, pp. 3054–3065, 1997.
- [3] V. Y. Bazhenov, M. S. Soskin, and M. V. Vasnetsov, Screw dislocations in light wavefronts, *J. Mod. Opt.*, vol. 39, no. 5, pp. 985–990, 1992.
- [4] L. Allen, M. W. Beijersbergen, R. J. C. Spreeuw, and J. P. Woerdman, Orbital angular momentum of light and the transformation of Laguerre-Gaussian laser modes, *Phys. Rev. A*, vol. 45, no. 11, pp. 8185–8189, Jun. 1992.
- [5] H. He, M. Firese, N. Heckenberg, and H. Rubinsztein-Dunlop, Optical particle trapping with higher-order doughnut beams produced using high efficiency computer generated holograms, *J. Mod. Opt.*, vol. 42, no. 1, pp. 217–223, 1995.
- [6] T. Kuga, Y. Torii, N. Shiokawa, T. Hirano, Y. Shimizu, and H. Sasada, Novel optical trap of atoms with a doughnut beam, *Phys. Rev. Lett.*, vol. 78, no. 25, pp. 4713–4716, 1999.
- [7] B. T. Hefner and P. Marston, An acoustical helicoidal wave transducer with applications for the alignment of ultrasonic and underwater systems, *J. Acoust. Soc. Am.*, vol. 106, no. 6, pp. 3313–3316, 1999.
- [8] J. Thomas and R. Marchiano, Pseudo angular momentum and topological charge conservation for nonlinear acoustical vortices, *Phys. Rev. Lett.*, vol. 91, no. 24, art. no. 244302, 2003.
- [9] K. Volke-Sepelveda, A. O. Santillan, and R. R. Boullosa, Transfer of angular momentum to matter from acoustical vortices in free space, *Phys. Rev. Lett.*, vol. 100, no. 2, art. no. 024302, 2008.
- [10] A. O. Santillan and K. Volke-Sepelveda, A demonstration of rotating sound waves in free space and the transfer of their angular momentum to matter, *Am. J. Phys.*, vol. 77, no. 3, pp. 209–215, 2009.
- [11] R. Marchiano and J.-L. Thomas, Doing arithmetic with nonlinear acoustical vortices, *Phys. Rev. Lett.*, vol. 101, no. 6, art. no. 064301, 2008.
- [12] B. Marston, Acoustical helicoidal waves and Laguerre-Gaussian beams: Applications to scattering and to angular momentum transport, *J. Acoust. Soc. Am.*, vol. 103, no. 5, p. 2971, 1998.
- [13] S. Meyer, A. Bernert, S. Ritsch, and M. Gspan, Optoacoustic generation of a helicoidal ultrasonic beam, *Acoust. Soc. Am.*, vol. 115, no. 3, pp. 1142–1146, 2004.
- [14] S. Wilson, R. Jourdain, Q. Zhang, and R. Dorey, New materials for micro-scale sensors and actuators: An engineering review, *Mater. Sci. Eng. R*, vol. 56, no. 1–6, pp. 1–129, 2007.
- [15] M. Dansachmuller, I. Mineev, P. Bartu, I. Graz, N. Arnold, and S. Bauer, Generation and detection of broadband airborne ultrasound with cellular ferroelectrets, *Appl. Phys. Lett.*, vol. 91, no. 22, art. no. 222906, 2007.
- [16] J. Ealo, F. Seco, C. Prieto, A. Jimenez, J. Roa, A. Koutsou, and J. Guevara, Customizable ultrasonic transducers based on electromechanical film, in *IEEE Ultrasonics Symp.*, 2008, pp. 879–882.
- [17] J. Ealo, F. Seco, and A. R. Jimenez, Broadband EMFi-based transducers for ultrasonic air applications, *IEEE Trans. Ultrason. Ferroelectr. Freq. Control*, vol. 55, no. 4, pp. 919–929, 2008.
- [18] E. Gálvez, Gaussian beams in the optics course, *Am. J. Phys.*, vol. 74, no. 4, pp. 355–361, 2006.
- [19] R. Piestun, Y. Y. Schechner, and J. Shamir, Propagation-invariant wave fields with finite energy, *J. Opt. Soc. Am. A*, vol. 17, no. 2, pp. 294–303, 2000.
- [20] M. Abramowitz and I. Stegun, *Handbook of Mathematical Functions*, 9th ed., Mineola, NY: Dover, 1970.
- [21] R. Marchiano and J.-L. Thomas, Synthesis and analysis of linear and nonlinear acoustical vortices, *Phys. Rev. E*, vol. 71, no. 6, art. no. 066616, 2005.
- [22] D. Placko and T. Kundu, *DPSM for Modeling Engineering Problems*. New York, NY: Wiley-Interscience, 2007.
- [23] J. Ealo, J. Camacho, and C. Fritsch, Airborne ultrasonic phased arrays using ferroelectrets: A new fabrication approach, *IEEE Trans. Ultrason. Ferroelectr. Freq. Control*, vol. 56, no. 4, pp. 848–858, 2009.



Joao L. Ealo is an Assistant Professor in the School of Mechanical Engineering of the University of Valle, Cali, Colombia. He was born in Cartagena de Indias, Colombia, in 1976. He received a B.Sc. degree in mechanical engineering from the University of Ibagu , Colombia, in 1998, and an M.Sc. degree in industrial control systems from the University of Valladolid, Spain in 2000. He obtained a Ph.D. degree in mechanical engineering from the Polytechnic University of Madrid, Spain, in 2009.

Since 2004, he has been a Researcher with the Instituto de Automaci3n Industrial, Consejo Superior de Investigaciones Cient ficas (CSIC), Madrid. His research interests are focused on localization systems, mainly those based on ultrasonic signals, with special emphasis on signal design and processing, positioning algorithms, robustness, standardization, optimal configurations, calibration methods, and development of new transducers.

His current research interests are aimed at exploring the potential of different transducer technologies to be used in air-coupled ultrasonic applications, such as acoustic imaging, nondestructive testing, material characterization, robot navigation, etc. This comprises the design, fabrication, modeling, and electro-mechanical-acoustical characterization of transducers.



Fernando Seco Granja was born in 1972 in Madrid, Spain. He holds a degree in physics (Universidad Complutense of Madrid, 1996) and a Ph.D. degree in physics (UNED, 2002), for which his dissertation dealt with the magnetostrictive generation of ultrasonic waves applied to a linear position sensor. Since 1997, he has been working at the Consejo Superior de Investigaciones Cient ficas (CSIC) in Arganda del Rey, Madrid, where he holds a research position.

His main research interest is in the design and development of indoor local positioning systems (LPS), especially those based on ultrasonic and radiofrequency technologies, in the modulation and coding of ultrasonic signals, and in Bayesian localization methods.



Jos  Carlos Prieto was born in Le3n, Spain, in 1978. He received a Technical degree in industrial electronics and a B.S. degree in electronics engineering from the Universidad de Extremadura, Badajoz, Spain, in 1999 and 2003, respectively, and a Master's degree in robotics from the Universidad Polit cnica de Madrid, Madrid, Spain, in 2007. He is currently working toward a Doctoral degree in robotics with the Universidad de Alcal , Madrid.